Synchronization of kinks in the two-lane totally asymmetric simple exclusion process with open boundary conditions

2005 J. Phys. A: Math. Gen. 38 3087

(http://iopscience.iop.org/0305-4470/38/14/002)

INSTITUTE OF PHYSICS PUBLISHING JOURNAL OF PHYSICS A: MATHEMATICAL AND GENERAL

J. Phys. A: Math. Gen. **38** (2005) 3087–3096 doi:10.1088/0305-4470/38/14/002

Synchronization of kinks in the two-lane totally asymmetric simple exclusion process with open boundary conditions

Tetsuya Mitsudo and Hisao Hayakawa

Department of Physics, Yoshida-South Campus, Kyoto University, Sakyo-ku, Kyoto 606-8501, Japan

E-mail: mitsudo@scphys.kyoto-u.ac.jp and hisao@yuragi.jinkan.kyoto-u.ac.jp

Received 31 December 2004, in final form 21 February 2005
Published 21 March 2005
Online at stacks.iop.org/JPhysA/38/3087

Abstract

We study the motion of kinks in a two-lane model of the totally asymmetric simple exclusion process with open boundaries. We analytically study the motion of the kinks by a decoupling approximation. In terms of the decoupling approximation, we find that the positions of the kinks become synchronized, though the difference in the number of particles between lanes remains non-zero when the rate of lane change is asymmetric. The validity of this result is confirmed for small asymmetric cases through the Monte Carlo simulation.

PACS numbers: 05.70.Ln, 45.70.Vn

1. Introduction

We often encounter congestion of pedestrian flows and traffic flows in our daily life. We also observe the sticking of grains in granular flows. It is important to study the mechanism of congestion not only from the industrial point of view but also from the physical point of view. For the sake of scientific research, we need to analyse a simple model which captures the essence of the phenomenon.

The asymmetric simple exclusion process (ASEP) is one of the simple models adequate to describe such a transport phenomenon [1, 2]. It is a stochastic system of particles moving asymmetrically on a lattice. The simplest limit of ASEP is that the particle is only allowed to hop in one direction, which is called the totally asymmetric simple exclusion process (TASEP).

It is known that the stationary state of one-lane ASEP under open boundary conditions has been obtained exactly [3–6]. Dynamical properties of TASEP are also studied expensively. The exact solutions of the master equation by Bethe ansatz on an infinite system [7] and a

periodic system [8] have been obtained. Furthermore, the current fluctuations in an infinite system and a semi-infinite system [9] are also studied. In the open boundary system, we can draw a phase diagram by the parameters of inflow rate and outflow rate at the boundaries. On the phase boundary between the low density phase and the high-density phase, there exists a diffusive domain wall (kink) [10–14]. Recently, Takesue *et al* [14] have derived a $f^{-3/2}$ law in the power spectrum as a function of the frequency f based on the random walk picture of the kink, and confirmed its quantitative validity from the comparison of the Monte Carlo simulation with their theoretical prediction.

However, we know little of the properties of a multi-lane ASEP which is more realistic than the one-lane model. There are several two-lane models of ASEP [15–18]. As used in [15] or [16], a realistic lane change rule should refer to the states of the front sites. However, the rule makes it difficult for us to analyse because we need to construct a transfer matrix to refer to the states of three or four sites, which are the current site, the front site and the side site, or the front site of another lane. Belitsky *et al* [15] successfully analysed the long-time properties of such the two-lane model in an infinite system. Here, we adopt a simpler model of lane change in which the particle may change lanes when the side site is vacant and do not refer to the front site. Although the two-lane (channel) model which adopts this simple rule is dealt by Pronina *et al* [18] who analysed the model based on a cluster approximation and compared the result with their extensive simulations, the lane change rates and the boundary parameters are symmetric in their model. We extend their model to the case of asymmetric lane change rule and boundary parameters to study a more general situation.

The purpose of this paper is to clarify the motion of kinks in a two-lane TASEP. To fulfil the analysis, we introduce our model and explain how to specify the position of the kink in the next section. In section 3, we discuss the motion of two kinks based on a decoupling (mean field) approximation. We find that the motions of the kinks are synchronized though the number of particles in one lane is different from that in another lane. We compare the solution with the results of Monte Carlo simulation. In section 4, we discuss the validity of the mean-field approximation. We find that the two-point correlation function is small during the relaxation process from the independent motion of two kinks to a synchronized motion of them. In section 5, we conclude our results.

2. Our model

2.1. Introduction of our two-lane model

Our two-lane model is defined on a two-lane lattice of $L \times 2$ sites, where L is the length of one lane. We introduce the occupation variable $\tau_{j;\ell}$ where $\tau_{j;\ell} = 1$ and $\tau_{j;\ell} = 0$ represent the occupied state and the vacant state on the jth site in the ℓth lane, respectively. The particle moves forward by the rate 1 during the time interval dt if the front site is vacant. We assume that all the particles drift from the left to the right. The open boundary condition is characterized by the inflow rate α_ℓ and the outflow rate β_ℓ. The particle is injected to the system by the rate α_ℓ when the first site in the ℓth lane is empty, while the particle is extracted from the system by the rate β_ℓ when the Lth site in the ℓth lane is occupied. On all sites, the particle is allowed to change lanes only to the neighbouring site. A particle on the 1st (2nd) lane can change lanes by the rate $r_\downarrow$ ($r_\uparrow$) when the side site in another lane is empty. (See figure 1 for a schematic explanation of the model.)

We denote the probability of finding the system in the configuration $\tau = \{\tau_{1;1}, \tau_{2;1}, \ldots, \tau_{L;2}\}$ by $P(\tau_{1;1}, \tau_{2;1}, \ldots, \tau_{L;2})$. We write the time evolution of the two-lane model

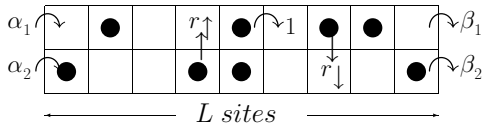

Figure 1. A sample picture of the two-lane model.

by the master equation,

$$\begin{aligned}\frac{\mathrm{d}}{\mathrm{d}t}P(\tau_{1;1},\ldots,\tau_{L;2}) &= \sum_{\sigma_{1;1}}(h_{1;1})_{\tau_{1;1};\sigma_{1;1}}P(\sigma_{1;1},\ldots,\tau_{L;2})\\ &+\sum_{\sigma_{1;2}}(h_{1;2})_{\tau_{1;2};\sigma_{1;2}}P(\tau_{1;1},\ldots,\sigma_{1;2},\ldots,\tau_{L;2})\\ &+\sum_{\ell=1}^{2}\sum_{j=1}^{L-1}\sum_{\sigma_{j;\ell},\sigma_{j+1;\ell}}(h_{j,j+1;\ell})_{\tau_{j;\ell},\tau_{j+1;\ell};\sigma_{j;\ell},\sigma_{j+1;\ell}}P(\tau_{1;1},\ldots,\sigma_{j;\ell},\sigma_{j+1;\ell},\ldots,\tau_{L;2})\\ &+\sum_{\sigma_{L;1}}(h_{L;1})_{\tau_{L;1};\sigma_{L;1}}P(\tau_{1;1},\ldots,\sigma_{L;1},\ldots,\tau_{L;2})\\ &+\sum_{\sigma_{L;2}}(h_{L;2})_{\tau_{L;2};\sigma_{L;2}}P(\tau_{1;2},\ldots,\sigma_{L;2})\\ &+\sum_{j=1}^{L}\sum_{\sigma_{j;1},\sigma_{j;2}}(h_{j;1,2})_{\sigma_{j;1},\sigma_{j;2};\tau_{j;1},\tau_{j;2}}P(\tau_{1;1},\ldots,\sigma_{j;1},\ldots,\sigma_{j;2},\ldots,\tau_{L;2})\end{aligned}\tag{1}$$

where $\sigma_{j;\ell}$ is used for a dummy variable in the summation, and the transition matrices $h_{1;\ell}, h_{L;\ell}, h_{j,j+1;\ell}, h_{j;1,2}$ are represented as

$$h_{1,\ell}=\begin{pmatrix}-\alpha_\ell & 0\\ \alpha_\ell & 0\end{pmatrix}_{1;\ell}\qquad h_{L,\ell}=\begin{pmatrix}0 & \beta_\ell\\ 0 & -\beta_\ell\end{pmatrix}_{L;\ell}$$

$$h_{j,j+1;\ell}=\begin{pmatrix}0&0&0&0\\0&0&1&0\\0&0&-1&0\\0&0&0&0\end{pmatrix}_{j,j+1;\ell}\qquad h_{j;1,2}=\begin{pmatrix}0&0&0&0\\0&-r_\uparrow&r_\downarrow&0\\0&r_\uparrow&-r_\downarrow&0\\0&0&0&0\end{pmatrix}_{j;1,2}.\tag{2}$$

Here the density function $\langle\tau_{j;\ell}\rangle$ and two-point function $\langle\tau_{j;\ell}\tau_{k;\ell'}\rangle$ are defined by

$$\langle\tau_{j;\ell}\rangle=\sum_{\tau}\tau_{j;\ell}P(\tau_{1;1},\ldots,\tau_{L;2})\tag{3}$$

$$\langle\tau_{j;\ell}\tau_{k;\ell'}\rangle=\sum_{\tau}\tau_{j;\ell}\tau_{k;\ell'}P(\tau_{1;1},\ldots,\tau_{L;2}),\tag{4}$$

where the summation is taken over all the configurations. The time evolution of $\langle\tau_{j;\ell}\rangle$ is written as

$$\frac{\mathrm{d}}{\mathrm{d}t}\langle\tau_{j;\ell}\rangle=J_{j-1,j;\ell}-J_{j,j+1;\ell}-J_{j;\ell\to\ell'}+J_{j;\ell'\to\ell}\tag{5}$$

for $\ell'\neq\ell$, where the current $J_{j,j+1;\ell}$ between site j and $j+1$ is

$$J_{j,j+1;\ell}=\langle\tau_{j;\ell}(1-\tau_{j+1;\ell})\rangle\tag{6}$$

and the currents between lanes are

$$J_{j;1\to 2} = r_\downarrow \langle \tau_{j;1}(1-\tau_{j;2})\rangle \qquad J_{j;2\to 1} = r_\uparrow \langle \tau_{j;2}(1-\tau_{j;1})\rangle. \tag{7}$$

2.2. The position of the kink

It is known that a kink appears when the inflow rate is equal to the outflow rate and both rates are smaller than 1/2 in one-lane ASEP. The kinks also appear in the two-lane model when $\alpha_1 = \beta_1 < 1/2$ and $\alpha_2 = \beta_2 < 1/2$. For $r_\uparrow \neq 0$ and $r_\downarrow \neq 0$, it is obvious that the motion of one kink depends on another kink.

We need to specify the position of the kinks in order to discuss their correlated motion. The position of a stable kink in the one-lane ASEP can be determined by using the second-class particle [10, 11]. However, we adopt another method to determine the position of the kink by the whole number of particles in a lane. This definition has been used in the domain wall theory [12–14], and gives the exact position of the kink when the inflow and outflow rates are small. The advantage to adopt this method is that it is much simpler than the method by the second-class particle.

We introduce $\langle N_\ell \rangle$ for the whole number of particles in each lane

$$\langle N_\ell \rangle = \sum_{j=1}^{L} \langle \tau_{j;\ell} \rangle. \tag{8}$$

We also introduce $\langle N_G \rangle$ and $\langle N_R \rangle$ by $\langle N_G \rangle = (\langle N_2 \rangle + \langle N_1 \rangle)/2$ and $\langle N_R \rangle = \langle N_2 \rangle - \langle N_1 \rangle$, respectively. The position of the kink x_ℓ is defined from the equation based on a kink picture

$$x_\ell = \frac{\langle N_\ell \rangle - \rho_{\ell;+} L}{\rho_{\ell;-} - \rho_{\ell;+}}, \tag{9}$$

where $\rho_{\ell;\pm}$ represent the density of the ℓth lane. The index + represents the right side of the position of the kink and index − represents the left side of the position of the kink. It is straightforward to give equation (9) by summing up the equation

$$\langle \tau_{j;\ell} \rangle = \rho_{\ell;-} + (\rho_{\ell;+} - \rho_{\ell;-})\theta(j - x_\ell) \tag{10}$$

from $j = 1$ to L, where $\theta(z)$ is the step function,

$$\theta(z) = \begin{cases} 1 & \text{for} \quad z \geqslant 0 \\ 0 & \text{for} \quad z < 0. \end{cases} \tag{11}$$

Thus, once $\langle N_\ell \rangle$ is known, we can determine the position of the kink.

3. Mean-field theory

For the large system size L, we can neglect the boundary terms. Thus, the equations for $\langle N_G \rangle$, $\langle N_R \rangle$ are given by

$$\frac{\mathrm{d}}{\mathrm{d}t}\langle N_G \rangle = 0 \tag{12}$$

$$\frac{\mathrm{d}}{\mathrm{d}t}\langle N_R \rangle = -2r_\uparrow \langle N_R \rangle + 2(r_\downarrow - r_\uparrow) \sum_{j=1}^{L} \langle \tau_{j;1}(1-\tau_{j;2})\rangle. \tag{13}$$

When $r_\downarrow = r_\uparrow$, equation (13) is reduced to

$$\frac{\mathrm{d}}{\mathrm{d}t}\langle N_R \rangle = -2r_\uparrow \langle N_R \rangle. \tag{14}$$

Thus $\langle N_R \rangle$ relaxes to 0 exponentially, and the number of particles becomes identical in both lanes in the long time limit.

However for $r_\downarrow \neq r_\uparrow$, the problem becomes nontrivial because of the two-point function in the second term in the right-hand side of equation (13). In general, the two-point correlation function is determined by an equation including three-point correlation function. Thus, we cannot obtain the exact form of the many-point correlation functions without truncation of the hierarchy of correlation functions. Here we adopt the simplest truncation, which is the decoupling (mean-field) approximation as

$$\sum_{j=1}^{L} \langle \tau_{j;1}(1-\tau_{j;2}) \rangle \simeq \sum_{j=1}^{L} \langle \tau_{j;1} \rangle (1 - \langle \tau_{j;2} \rangle). \tag{15}$$

We also use the kink picture (10) to approximate the density profile $\langle \tau_{j;\ell} \rangle$.

Let us discuss the motion of two kinks starting from the initial condition where two separated kinks exist in both lanes. The density profile changes in time during the synchronization of the kinks. Furthermore, we assume that the density changes by keeping the density profile (10). Thus, we have to determine the time evolution of the density $\rho_{\ell;\pm}$ on the both sides of the kink. By introducing $\rho_{G;\pm} = \frac{\rho_{2;\pm}+\rho_{1;\pm}}{2}$ and $\rho_{R;\pm} = \rho_{2;\pm} - \rho_{1;\pm}$, the time evolution equations for $\rho_{G;\pm}$ and $\rho_{R;\pm}$ are, respectively, written as

$$\frac{\mathrm{d}}{\mathrm{d}t}\rho_{G;\pm} = 0 \tag{16}$$

$$\frac{\mathrm{d}}{\mathrm{d}t}\rho_{R;\pm} = -(r_\uparrow + r_\downarrow)\rho_{R;\pm} + \frac{1}{2}(r_\downarrow - r_\uparrow)\rho_{R;\pm}^2 + (r_\downarrow - r_\uparrow)\big(\rho_{G;\pm} - \rho_{G;\pm}^2\big). \tag{17}$$

Equations (16) and (17) can be solved exactly,

$$\rho_{G;\pm} = \rho_{G;\pm}^0 \tag{18}$$

$$\rho_{R;\pm} = \omega_- + \frac{2\gamma}{\epsilon}\frac{\mathrm{e}^{-\gamma t}}{\mathrm{e}^{-\gamma t} - C_\pm}, \tag{19}$$

where

$$\epsilon = r_\downarrow - r_\uparrow \qquad \gamma = \frac{1}{2}(r_\downarrow - r_\uparrow)(\omega_+ - \omega_-) \tag{20}$$

$$\omega_\pm = \frac{r_\downarrow + r_\uparrow \pm \sqrt{(r_\downarrow + r_\uparrow)^2 - 2(r_\downarrow - r_\uparrow)^2(\alpha_1 + \alpha_2 - (\alpha_1+\alpha_2)^2/2)}}{r_\downarrow - r_\uparrow} \tag{21}$$

$$C_\pm = \frac{\rho_{R;\pm}^0 - \omega_+}{\rho_{R;\pm}^0 - \omega_-}. \tag{22}$$

The initial conditions $\rho_{G;\pm}^0$ and $\rho_{R;\pm}^0$ are taken as the stationary densities in one-lane model as

$$\rho_{G;-}^0 = \frac{\alpha_1 + \alpha_2}{2} \qquad \rho_{R;-}^0 = \alpha_2 - \alpha_1 \tag{23}$$

$$\rho_{G;+}^0 = \frac{2 - \alpha_1 - \alpha_2}{2} \qquad \rho_{R;+}^0 = \alpha_1 - \alpha_2. \tag{24}$$

Thus, we obtain the density $\rho_{\ell;-}$

$$\rho_{1;-} = \rho_1' - \frac{\gamma}{\epsilon}\frac{\mathrm{e}^{-\gamma t}}{\mathrm{e}^{-\gamma t} - C_-} \qquad \rho_{2;-} = \rho_2' + \frac{\gamma}{\epsilon}\frac{\mathrm{e}^{-\gamma t}}{\mathrm{e}^{-\gamma t} - C_-} \tag{25}$$

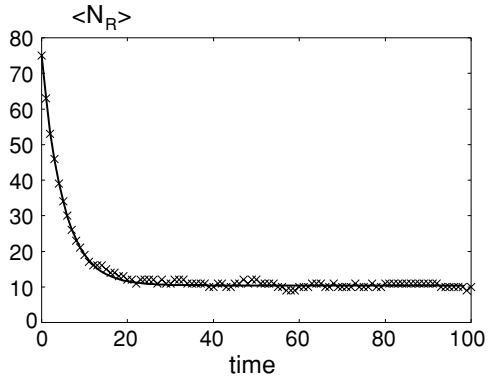

Figure 2. The comparison of time evolution between the simulation and the calculation. The solution (A.4) is shown by the solid line and the simulation result is shown by the crosses (×). The parameters are $\alpha_1 = \beta_1 = 0.1, \alpha_2 = \beta_2 = 0.15, r_\downarrow = 0.11, r_\uparrow = 0.1, L = 1000$. Time step is taken for each Monte Carlo step. The initial condition is fixed to $\langle N_R \rangle_0 = 75$ and averaged over 1000 samples.

and the density $\rho_{\ell;+}$

$$\rho_{1;+} = 1 - \rho_2' - \frac{\gamma}{\epsilon}\frac{\mathrm{e}^{-\gamma t}}{\mathrm{e}^{-\gamma t} - C_+} \qquad \rho_{2;+} = 1 - \rho_1' + \frac{\gamma}{\epsilon}\frac{\mathrm{e}^{-\gamma t}}{\mathrm{e}^{-\gamma t} - C_+} \tag{26}$$

where

$$\rho_1' = \frac{\alpha_1 + \alpha_2 - \omega_-}{2} \qquad \rho_2' = \frac{\alpha_1 + \alpha_2 + \omega_-}{2}. \tag{27}$$

Therefore, we obtain the time evolution of the density profile $\langle \tau_{j;\ell} \rangle$ for $r_\downarrow \neq r_\uparrow$.

Substituting equation (10) into (13) with the aid of (15), we obtain

$$\frac{\mathrm{d}}{\mathrm{d}t}\langle N_R \rangle = -(2r_\uparrow + \epsilon(1 - \rho_{2;-} + \rho_{1;+}))\langle N_R \rangle + 2\epsilon(\rho_{1;+}\rho_{2;-}L + (1 - \rho_{1;+} - \rho_{2;-})\langle N_G \rangle) \tag{28}$$

for $x_1 < x_2$ and

$$\frac{\mathrm{d}}{\mathrm{d}t}\langle N_R \rangle = -(2r_\uparrow + \epsilon(1 - \rho_{2;+} + \rho_{1;-}))\langle N_R \rangle + 2\epsilon(\rho_{1;-}\rho_{2;+}L + (1 - \rho_{1;-} - \rho_{2;+})\langle N_G \rangle) \tag{29}$$

for $x_1 > x_2$. Equations (28) and (29) can be solved exactly, though the expression is lengthy (see (A.4) and (A.5)). Here, we present the solution for $\langle N_R \rangle$ in the long time limit as

$$\langle N_R \rangle_\infty = \frac{\epsilon\rho_1'(1 - \rho_1')L}{r_\uparrow + \epsilon\rho_1'} \tag{30}$$

for $x_1 > x_2$, and

$$\langle N_R \rangle_\infty = \frac{\epsilon\rho_2'(1 - \rho_2')L}{r_\downarrow - \epsilon\rho_2'} \tag{31}$$

for $x_1 < x_2$. These results show that there remains the mean difference of the number of particles between lanes. The validity of our analysis based on the decoupling approximation is confirmed by the comparison of our result with the Monte Carlo simulation when $|r_\uparrow - r_\downarrow|$ is not large. Figure 2 shows the quantitative accuracy of our analysis in the time evolution of $\langle N_R \rangle$.

Though $\langle N_R \rangle$ remains finite, the positions of the kinks are synchronized. In fact, from equations (30) or (31) and (9), we obtain

$$x_2 - x_1 = 0. \tag{32}$$

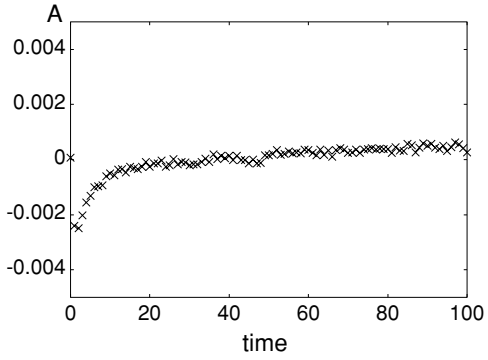

Figure 3. The time evolution of the value A from the simulation. The parameters used in this simulation are the same as those used in figure 2.

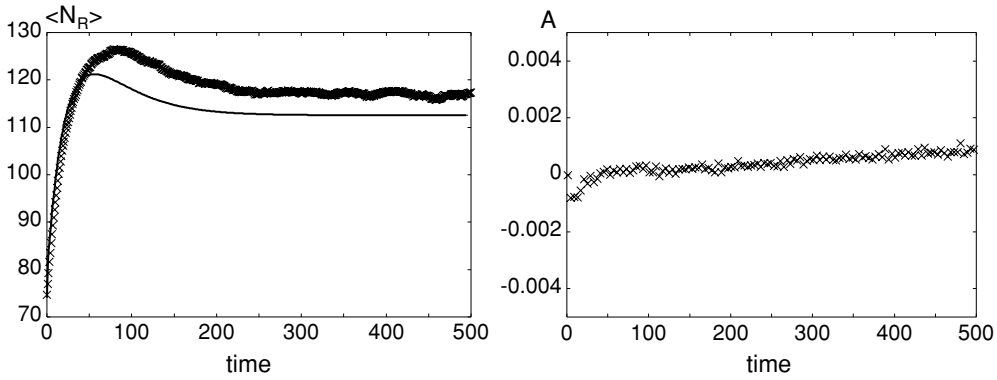

Figure 4. Left: the comparison of time evolution between the simulation and the calculation. The solution (A.4) is shown by the solid line and the simulation result is shown by the crosses ($\times$). Right: the time evolution of the value A from the simulation. In both figures, the parameters are $\alpha_1 = \beta_1 = 0.1, \alpha_2 = \beta_2 = 0.15, r_\downarrow = 0.03, r_\uparrow = 0.01, L = 1000$. Time step is taken for each Monte Carlo step. The initial condition is fixed to $\langle N_R \rangle_0 = 75$ and averaged over 1000 samples.

Thus, the positions of the kinks become identical in the long time limit. This result is reasonable, because we cannot choose a preferable congestion front in traffic jams.

4. Discussion

Now let us discuss the validity of the decoupling approximation. Although it is difficult to evaluate the two-point function exactly, it is possible to evaluate it from the Monte Carlo simulation. The result of our simulation for the two-point function

$$A = \frac{\sum_{j=1}^{L} \langle \tau_{j;1} \tau_{j;2} \rangle - \sum_{j=1}^{L} \langle \tau_{j;1} \rangle \langle \tau_{j;2} \rangle}{\sum_{\ell=1}^{2} \sum_{j=1}^{L} \langle \tau_{j;\ell}^2 \rangle} \tag{33}$$

is shown in figure 3 for the same parameters as used in figure 2, where we realize that A is small between $t = 30$ and $t = 100$. The synchronization is realized before $t = 30$ as we can see in figure 2. Thus, we may expect that the decoupling approximation adopted here works well to describe the synchronization of the kinks.

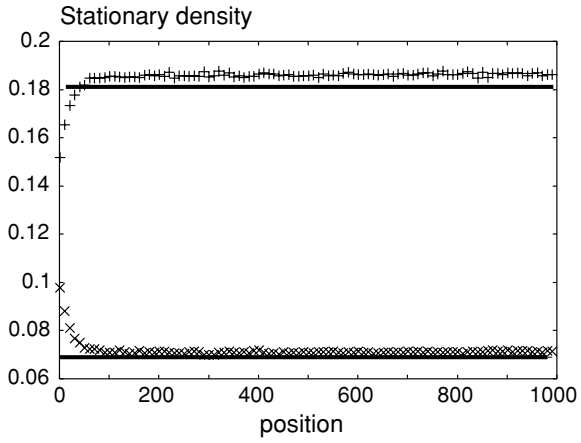

Figure 5. The difference between the stationary density given by the simulation and that by equation (17) in the corresponding low-density region. The symbols (+) stand for the first lane, the symbols (×) stand for the density in the second lane and the approximation is shown by the solid line. The boundary parameters are $\alpha_1 = 0.1, \beta_1 = 0.9, \alpha_2 = 0.15, \beta_2 = 0.85$, $r_\downarrow = 0.03, r_\uparrow = 0.01, L = 1000$.

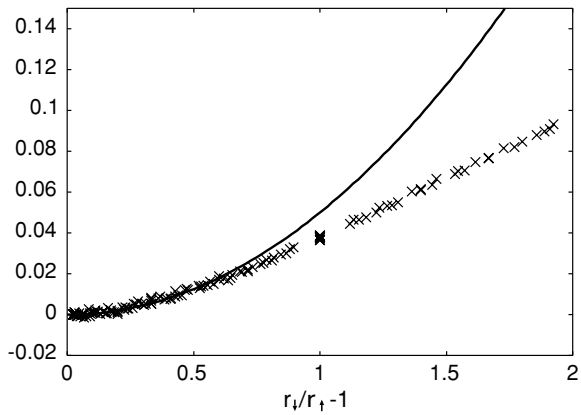

Figure 6. The final difference between the kink positions given by the simulation and the analysis. The crosses (×) show the difference and the solid line is the guideline which is proportional to $(\frac{r_\downarrow}{r_\uparrow} - 1)^2$. The boundary parameters are $\alpha_1 = \beta_1 = 0.1, \alpha_2 = \beta_2 = 0.15$, $L = 1000$.

However there is a certain parameter region that the decoupling approximation fails. In fact, the left figure in figure 4 shows $\langle N_R \rangle$ obtained from the simulation deviates from that in the decoupling approximation. The positions of the kinks are not identical in this case. The value A given by the simulation in the right figure in figure 4 when it deviates from the decoupling approximation. The value A is almost 0 in the region between $t = 30$ and $t = 200$. In such a region the stationary density $\rho_{\ell;\pm}$ is not given by equation (17). The comparison of $\rho_{\ell;-}$ between the result of the simulation and the solution of equation (17) is shown in figure 5. We can see that the density derived from the mean-field theory deviates from the result of the simulation. Thus, in the region where the final densities of each lane differ from the solutions of equation (17), the final positions of the kinks are not identical.

To verify the valid region of the decoupling approximation, in figure 6, we plot the deviation from the decoupling approximation in the difference between two kinks as a function of $r_\downarrow/r_\uparrow - 1$. From figure 6, we find that the deviation is proportional to $\delta^2 = (r_\downarrow/r_\uparrow - 1)^2$ for the small asymmetric cases. This is an interesting result, because the decoupling approximation predicts $\langle N_R\rangle \propto \delta$. Namely, the decoupling approximation can be used when we can regard δ as finite but δ^2 as negligible. In addition, the curvature of the parabola is relatively small, which ensures that we may use the approximation in $\delta < 0.2$. The quantitative analysis of the violation of the decoupling approximation will be a future problem.

5. Conclusion

In this paper, we have studied the motion of kinks in the two-lane TASEP. We obtain the explicit time evolution function of the average number of particles in each lane which is related to the position of the kink by adopting the decoupling approximation of the two-point correlation function. We find that the positions of the kinks are synchronized, though the number of particles in a lane can be different from that in another lane. We confirm the validity of our analysis by comparing the result of the Monte Carlo simulation and the analytical result. The deviation from the mean-field analysis is small when the lane change rates are nearly symmetric.

Acknowledgments

We would like to thank S Takesue for fruitful discussion. This work is partially supported by the grant-in-aid for Scientific Research (grant no. 15540393) of the Ministry of Education, Culture, Sports, Science and Technology (MEXT), Japan, and the grant-in-aid for the 21st century COE 'Center for Diversity and Universality in Physics' from MEXT, Japan.

Appendix. The calculation of $\langle N_R\rangle$

In this appendix, we give the explicit expression of $\langle N_R\rangle$. Equation (29) is solved as

$$\begin{aligned}\langle N_R\rangle = \langle N_R\rangle_0 \exp\left(-\int_0^t \mathrm{d}t'(2r_\uparrow + \epsilon(1-\rho_{2;+}+\rho_{1;-}))\right)\\ +\epsilon\int_0^t \mathrm{d}t' \exp\left(\int_t^{t'} \mathrm{d}t''(2r_\uparrow+\epsilon(1-\rho_{2;+}+\rho_{1;-}))\right)\\ \times(2L\rho_{1;-}\rho_{2;+} + 2(1-\rho_{1;-}-\rho_{2;+})\langle N_G\rangle).\end{aligned} \tag{A.1}$$

Here, we perform the integral in the argument of the exponential function

$$\int_0^t \mathrm{d}t'(1-\rho_{2;+}+\rho_{1;-}) = 2\rho_1' t + \frac{1}{\epsilon}\ln\left(\frac{(C_+ - \mathrm{e}^{-\gamma t})(C_- - \mathrm{e}^{-\gamma t})}{C_+C_-}\right). \tag{A.2}$$

Therefore,

$$\exp\left(-\int_0^t \mathrm{d}t'(2r_\uparrow+\epsilon(1-\rho_{2;+}+\rho_{1;-}))\right) = \exp(-2(r_\uparrow+\epsilon\rho_1')t)\frac{C_+C_-}{(C_+-\mathrm{e}^{-\gamma t})(C_- - \mathrm{e}^{-\gamma t})}. \tag{A.3}$$

After executing the calculation, we finally achieve

$$\begin{aligned}\langle N_R\rangle = \langle N_R\rangle_0 \exp(-2(r_\uparrow+\epsilon\rho_1')t)\frac{C_+C_-}{(C_+-\mathrm{e}^{-\gamma t})(C_--\mathrm{e}^{-\gamma t})}+\frac{\epsilon}{(C_+-\mathrm{e}^{-\gamma t})(C_--\mathrm{e}^{-\gamma t})}\\ \times\left[L\rho_1'(1-\rho_1')C_+C_-\frac{1-\exp(-2(r_\uparrow+\epsilon\rho_1'))}{r_\uparrow+\epsilon\rho_1'}+\frac{\mathrm{e}^{-\gamma t}-\exp(-2(r_\uparrow+\epsilon\rho_1'))}{2(r_\uparrow+\epsilon\rho_1')-\gamma}\right.\\ \times 2L\left(\frac{\gamma}{\epsilon}(C_+-\rho_1'(C_-+C_+))-(C_-+C_+)\rho_1'(1-\rho_1')\right)\\ +\frac{\mathrm{e}^{-\gamma t}-\exp(-2(r_\uparrow+\epsilon\rho_1'))}{2(r_\uparrow+\epsilon\rho_1')-\gamma}\frac{2\gamma}{\epsilon}(C_--C_+)\langle N_G\rangle\\ \left.+\frac{\mathrm{e}^{-2\gamma t}-\exp(-2(r_\uparrow+\epsilon\rho_1'))}{r_\uparrow+\epsilon\rho_1'-\gamma}\left(-\frac{\gamma^2}{\epsilon^2}+\frac{\gamma}{\epsilon}(2\rho_1'-1)+\rho_1'(1-\rho_1')\right)L\right]\end{aligned}\tag{A.4}$$

for $x_1 > x_2$, and

$$\begin{aligned}\langle N_R\rangle = \langle N_R\rangle_0 \exp(-2(r_\downarrow-\epsilon\rho_2')t)\frac{C_+C_-}{(C_+-\mathrm{e}^{-\gamma t})(C_--\mathrm{e}^{-\gamma t})}+\frac{\epsilon}{(C_+-\mathrm{e}^{-\gamma t})(C_--\mathrm{e}^{-\gamma t})}\\ \times\left[L\rho_2'(1-\rho_2')C_-C_+\frac{1-\exp(-2(r_\downarrow-\epsilon\rho_2'))}{r_\downarrow-\epsilon\rho_2'}+\frac{\mathrm{e}^{-\gamma t}-\exp(-2(r_\downarrow-\epsilon\rho_2'))}{2(r_\downarrow-\epsilon\rho_2')-\gamma}\right.\\ \times 2L\left(\frac{\gamma}{\epsilon}(C_++\rho_2'(C_--C_+))-(C_-+C_+)\rho_2'(1-\rho_2')\right)\\ +\frac{\mathrm{e}^{-\gamma t}-\exp(-2(r_\downarrow-\epsilon\rho_2'))}{2(r_\downarrow-\epsilon\rho_2')-\gamma}\frac{2\gamma}{\epsilon}(C_--C_+)\langle N_G\rangle\\ \left.+\frac{\mathrm{e}^{-2\gamma t}-\exp(-2(r_\downarrow-\epsilon\rho_2'))}{r_\downarrow-\epsilon\rho_2'-\gamma}\left(-\frac{\gamma^2}{\epsilon^2}+\frac{\gamma}{\epsilon}(2\rho_2'-1)+\rho_2'(1-\rho_2')\right)L\right]\end{aligned}\tag{A.5}$$

for $x_1 < x_2$.

References

[1] Schütz G M 2001 Exact solvable models for many-body systems far from equilibrium *Phase Transitions and Critical Phenomena* vol 19, ed C Domb and J L Lebowitz (London: Academic)
[2] Schmittmann B and Zia R K P 1994 Statistical mechanics of driven diffusive systems *Phase Transitions and Critical Phenomena* vol 17, ed C Domb and J L Lebowitz (London: Academic)
[3] Derrida B, Evans M R, Hakeem V and Pasquier V 1993 *J. Phys. A: Math. Gen.* **26** 1493
[4] Schütz G M and Domany E 1993 *J. Stat. Phys.* **72** 277
[5] Sasamoto T 1999 *J. Phys. A: Math. Gen.* **32** 7109
[6] Uchiyama M, Sasamoto S and Wadati M 2004 *J. Phys. A: Math. Gen.* **37** 4985
[7] Schütz G M 1997 *J. Stat. Phys.* **88** 427
[8] Priezzhev V B 2003 *Phys. Rev. Lett.* **91** 050601
[9] Prähofer M and Spohn H 2002 *In and Out of Equilibrium* vol 51, ed V Sidoravicious p 185
[10] Derrida B, Lebowitz J L and Speer E R 1997 *J. Stat. Phys.* **89** 135
[11] Ferrari P A 1992 *Prob. Theor. Rel. Fields* **91** 81
[12] Kolomeisky A B, Schütz G M, Kolomeisky E B and Straley J P 1998 *J. Phys. A: Math. Gen.* **31** 6911
[13] Santen L and Appert C 2002 *J. Stat. Phys.* **106** 187
[14] Takesue S, Mitsudo T and Hayakawa H 2003 *Phys. Rev.* E **68** 015103(R)
[15] Belitsky V, Krug J, Neves E J and Schütz G M 2001 *J. Stat. Phys.* **103** 945
[16] Nagatani T 1996 *J. Phys. A: Math. Gen.* **29** 6531
[17] Popkov V and Schütz G M 2003 *J. Stat. Phys.* **112** 523
[18] Pronina E and Kolomeisky A B 2004 *J. Phys. A: Math. Gen.* **37** 9907